

Tamm minibands in superlattices

S. G. Tikhodeev

Institute of General Physics, USSR Academy of Sciences

(Submitted 8 February 1991)

Zh. Eksp. Teor. Fiz. **99**, 1871–1880 (June 1991)

The properties of interface (Tamm) minibands in superlattices are investigated using a simple exactly-solvable one-dimensional model. Tamm minibands originate from states that are localized at the boundaries of different layers; they appear in pairs (when the spectra of the individual layers are nondegenerate) as a result of the interaction of Tamm levels belonging to adjacent interfaces. It is shown that a correct description of these minibands within the framework of the envelope approximation must incorporate into the boundary conditions the fact that the band-edge Bloch functions of the layers in contact are different. An exception is the case where inverted bands overlap, in which case the Tamm minibands are insensitive to the boundary conditions.

One of the most interesting problems in the physics of semiconductor structures and superlattices is that of interface states, i.e., spatially localized states at the boundaries between layers. For an isolated interface these states, referred to as Tamm states,¹ are located in energetically forbidden regions of the contacting materials. In a superlattice with sufficiently thin layers, Tamm states that are localized in adjacent interfaces must broaden into "Tamm minibands." Although these states were discussed in the literature long ago (see, e.g., Refs. 2–4), their nature remains obscure. Only for the case of interfaces involving inverted bands (such as, e.g., structures based on HgTe–CdTe) are these interface states stable with respect to variations in the near surface potential.⁵ Because the inverted-band interface is the only one whose investigation involves easy calculations, even within the envelope approximation,³ it is also the only case that has been investigated with any degree of thoroughness.

In view of these assertions, it is useful to study the genesis of interface states and minibands for simple exactly-solvable models. Such models have been proposed in the literature. For example, Ref. 6 contains an investigation of interface states between two one-dimensional Kronig–Penney lattices. A closely related problem—that of states bound to defects in a superlattice—was discussed in Ref. 7 as well, again based on the Kronig–Penney model. In recent times these states have been investigated experimentally for a model structure consisting of a barrier and a collection of quantum wells⁸ (see also Refs. 9 and 10). However, to this author's knowledge there has been no attempt to use these models to investigate interface states that are intrinsic to the superlattices. (The use of semiconductor structures to model interface minibands, as in Ref. 8, requires that we deal with superlattices made of superlattices, i.e., in essence, with "super-superlattices.")

In Ref. 11 a simple exactly solvable superlattice model was described, made up of one-dimensional Kronig–Penney lattices with δ -function potentials, in which Tamm minibands can arise under certain conditions. For inverted bands (which are very easy to simulate in this model) these minibands appear independent of the overlap of the lattice forbidden bands. This agrees precisely with the results of Refs. 3 and 5. For overlapping noninverted bands, Tamm minibands appear when the band-edge Bloch functions differ suf-

ficiently, and disappear with increasing offset energy between the corresponding bands. Thus, a necessary condition for the appearance of Tamm interface states is that the Bloch functions at the band edges in the contacting layers be different.

This article contains a more detailed exposition of the results obtained in Ref. 11, as well as a comparison of the exact solution with the solution obtained within the envelope-function approximation, which is the most commonly used method in the theory of superlattices. (A review of the envelope method can be found, e.g., in Ref. 12.) In this paper it is shown that the assertion often made in the literature (see, e.g., Ref. 4) that interface states cannot be obtained by means of the envelope approximation in the absence of band inversion does not correspond to reality. Tamm minibands can be described with good accuracy within the envelope approximation if the change in the Bloch functions at the band edges of the contacting layers is built into the boundary conditions. In the most commonly used boundary conditions,¹³ which are derived from the requirement of conservation of current in the effective mass approximation, discontinuities in the Bloch (envelope) functions are neglected. This results in loss of the Tamm minibands except for the single case of inverted bands.^{3,5}

1. SUPERLATTICE MODEL AND EXACT SOLUTION

It is well known that the simplest model of a solid is the one-dimensional Kronig–Penney problem with a periodic potential $V + p\delta(\{x\})$. (Here $\{x\}$ is the fractional part of x . In what follows we will use a system of units with $\hbar = m = 1$ and assume unit spacing between the δ functions.) The spectrum of allowed states $E = E(k)$ for such a lattice is determined by the equation

$$\cos k = \cos \xi + \frac{p}{\xi} \sin \xi \quad (1)$$

(where $\xi = [2(E - V)]^{1/2}$) and consists of alternating allowed and forbidden bands. If $p > 0$, the points $\xi = \pi n$, $n = 1, 2, \dots$ (i.e., $E = V + \pi^2 n^2 / 2$) mark the lower boundaries of the forbidden bands (for $p < 0$ they are upper boundaries). In what follows we will refer to these forbidden bands as $n\pi$ gaps.

Let us construct a one-dimensional superlattice out of two different δ -function Kronig–Penney lattices (types A

and B), in which layers with N_a and N_b δ -functions of each type alternate. This superlattice is described by the Schrödinger equation

$$-\frac{1}{2}\Psi''(x) + V(x)\Psi(x) = E\Psi(x) \quad (2)$$

with a potential (see Fig. 1)

$$V(x) = \begin{cases} p_a\delta(\{x\}), & 0 \leq x \leq N_a \\ V_b + p_b\delta(\{x\}), & N_a < x < D \end{cases} \quad (3)$$

(for a single period $D = N_a + N_b$ of the superlattice); for simplicity the "interatomic" spacings in lattices A and B are taken to be the same. The parameter V_b allows us to shift the spectra of lattices A and B with respect to one another (in energy) and thereby to model different types of band overlap, i.e., superlattices of different types. Furthermore, if $p_a p_b < 0$ holds, we can model contacts with inverted bands.

Tamm states for isolated interfaces were studied recently in Ref. 6 within the framework of a model analogous to this one. For the case of overlapping $2n\pi$ gaps, the energy of

the Tamm state of an isolated interface can be found from the equation

$$\frac{\xi_a}{\sin \xi_a} \operatorname{sh} \chi_a + \frac{\xi_b}{\sin \xi_b} \operatorname{sh} \chi_b = p_b - p_a, \quad (4)$$

where $\chi = |\operatorname{Im} k|$ is the imaginary quasimomentum (i.e., the solution to Eq. (1) within the gap). For example, for $p_b < p_a < 0$, a Tamm state appears near the lower edges of the 2π gaps when these edges coincide, and disappears as the offset between bands increases. However, for $p_a p_b < 0$ the model describes an interface with inverted bands, and the Tamm state appears at the center of the overlapping 2π gaps. In a superlattice the interaction between states of adjacent interfaces leads to lifting of their degeneracy and splitting of the levels into two Tamm minibands. When the bare lattice spectra are nondegenerate, which is characteristic of the 1D situation, this splitting is a completely general topological property. In the 3D case the situation can be much more complicated.

For the Schrödinger equation with the superlattice potential (3) the eigensolution corresponding to the energy E has the following form within the interval $0 < x < D$:

$$\Psi(x) = \begin{cases} A_0 \exp(-i\xi_a \{x\}) + B_0 \exp(i\xi_a \{x\}), & 0 < x < 1 \\ \dots \\ A_{N_a-1} \exp(-i\xi_a \{x\}) + B_{N_a-1} \exp(i\xi_a \{x\}), & N_a-1 < x < N_a \\ A_{N_a} \exp(-i\xi_b \{x\}) + B_{N_a} \exp(i\xi_b \{x\}), & N_a < x < N_a+1 \\ \dots \\ A_{D-1} \exp(-i\xi_b \{x\}) + B_{D-1} \exp(i\xi_b \{x\}), & D-1 < x < D \end{cases} \quad (5)$$

Here

$$\begin{pmatrix} A_m \\ B_m \end{pmatrix} = T_m \begin{pmatrix} A_0 \\ B_0 \end{pmatrix}, \quad (6)$$

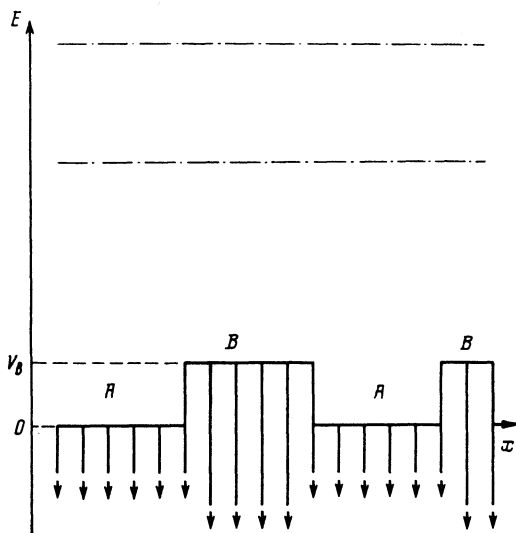


FIG. 1. Superlattice potential (δ -functions are shown as vertical arrows). The region of energies where we expect the superlattice spectrum to be is located between the dot-dashed lines in the upper part of the figure.

where the transfer matrix T_m is a product of the m transition matrices t_{aa} , t_{ab} , t_{bb} , and t_{ba} between adjacent δ -functions:

$$T_m = \begin{cases} (t_{aa})^m, & 1 \leq m \leq N_a-1 \\ (t_{bb})^{m-N_a} t_{ba} (t_{aa})^{N_a-1}, & N_a \leq m \leq D-1 \\ t_{ab} (t_{bb})^{N_b-1} t_{ba} (t_{aa})^{N_a-1}, & m=D \end{cases} \quad (7)$$

For example,

$$t_{ba} = \begin{pmatrix} \frac{1}{2} \left(1 + \frac{\xi_a}{\xi_b} \right) + \frac{i p_a}{\xi_b} & \frac{1}{2} \left(1 - \frac{\xi_a}{\xi_b} \right) + \frac{i p_a}{\xi_b} \\ \frac{1}{2} \left(1 - \frac{\xi_a}{\xi_b} \right) - \frac{i p_a}{\xi_b} & \frac{1}{2} \left(1 + \frac{\xi_a}{\xi_b} \right) - \frac{i p_a}{\xi_b} \end{pmatrix} \times \begin{pmatrix} e^{-i\xi_a} & 0 \\ 0 & e^{i\xi_a} \end{pmatrix}. \quad (8)$$

The matrices t_{aa} and t_{bb} are obtained from (8) by the replacement $b \rightarrow a$ and $a \rightarrow b$ respectively, while the matrix t_{ab} is obtained by making the replacement $a \leftrightarrow b$ in the $\xi_{a,b}$ alone (this asymmetry is associated with the choice of identical δ -functions for the interfaces).

The solution on the entire x axis is obtained from the Bloch condition

$$\Psi(x+D) = e^{iK D} \Psi(x), \quad (9)$$

and the dispersion relation $E = E(K)$ for the superlattices is

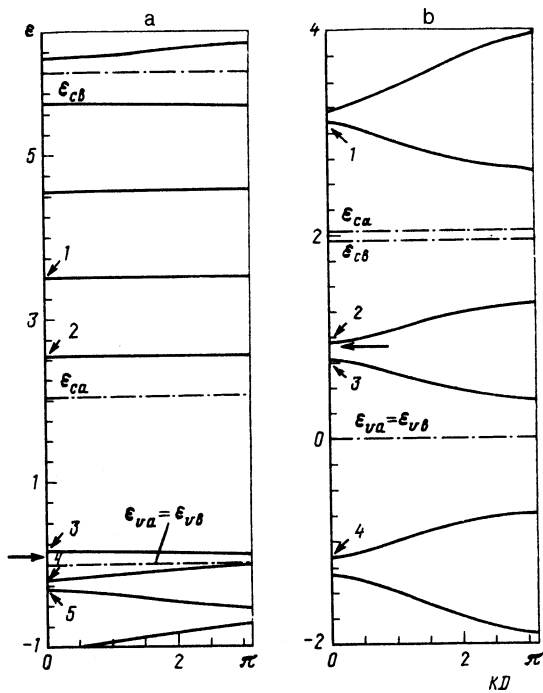


FIG. 2. Spectrum of model superlattices for $N_a = N_b = 15$, $p_a = -1$, $p_b = -3$ (a) and for $N_a = N_b = 10$, $p_a = -1$, $p_b = 1$ (b); the slanted arrows are used to denote the values of ε and $K = 0$ for which the functions shown in Fig. 3 were calculated. The horizontal arrows point to the position of the Tamm level of the isolated interface.

given by an equation analogous to Eq. (1):

$$\cos \kappa D = \frac{1}{2} \text{Tr } T_D \quad (10)$$

[Eq. (1) is obtained from Eq. (10) if we replace T_D by t_{aa} or t_{bb} in it].

Typical spectra and eigenfunctions (for $K = 0$ these are calculated using Eqs. (10) and (5) for the case where the 2π gaps overlap) are shown in Fig. 2 and Fig. 3 respectively. The cases shown are for no band inversion (a) and with inversion (b). The values of V_b are chosen so that the lower edges of the 2π gaps of lattices A and B coincide exactly. Energies in Fig. 2 are measured from this particular value;

the levels $\varepsilon_{v(c)a}$ and $\varepsilon_{v(c)b}$ denoted in Fig. 2 by the dashed lines are the lower (upper) boundaries of the 2π gaps for lattices A and B respectively. The horizontal arrows in these figures denote the positions of the Tamm levels calculated using Eq. (4) for the respective isolated interfaces.

Let us first consider the case of an interface without band inversion [Fig. 2(a) and Fig. 3(a)]. Four minibands lying in the energy region $\varepsilon_{ca} < \varepsilon < \varepsilon_{cb}$ are formed by states that are localized in the corresponding quantum wells (i.e., in layers of the more narrow band lattice A). This is obvious from Fig. 3a, where we show the wave functions of the two lower minibands (curves 1 and 2). As for the two minibands near the coincident "valence" band edges (curves 3 and 4), they are Tamm states, and arise as a consequence of the interaction between Tamm states localized on adjacent interfaces.

We note the following interesting circumstance. Although the lower Tamm miniband in Fig. 2a (curve 4) lies entirely within an allowed region common to the bare spectra of both lattices, the wave functions are localized at the interfaces. Whereas the quantity $\chi_{a,b}$ determines the extent to which the upper level is localized, for the lower level the localization is determined by interference and depends on $N_{a,b}$.¹⁾ We will continue our discussion of the properties of this miniband in the next section.

For $p_a p_b < 0$ (Figs. 2b and 3b) the inverted bands join smoothly, and the Tamm state is found at the center of the overlapping gaps. This situation has been analyzed in detail in the literature.^{3,5} For the superlattice the interaction of the interfaces leads to the formation of pairs of Tamm minibands (curves 2 and 3).

2. ENVELOPE FUNCTION APPROXIMATION

Because the superlattice model under discussion here admits an exact solution (a rare case), the use of this solution to investigate the approximations that are commonly used in calculations of superlattice band spectra is very productive. Here we will discuss the simplest and most often used approximation, the method of envelope functions. For a detailed review of this method see Ref. 12. In the envelope approximation the wave function is sought in the form of products of rapidly-varying band-edge Bloch functions

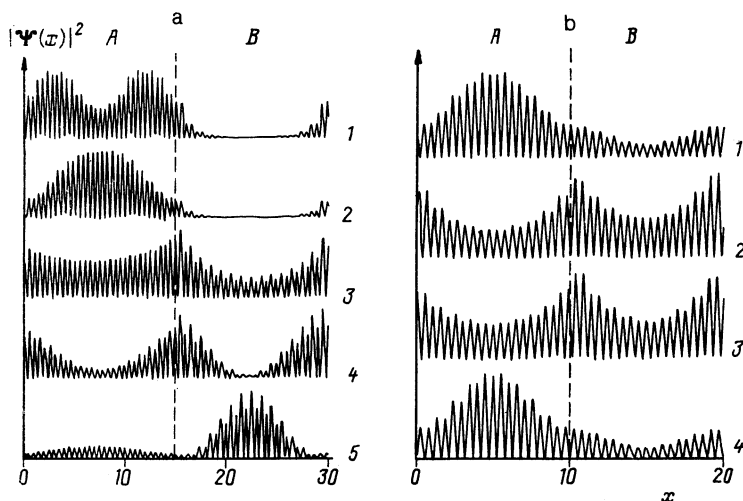


FIG. 3. Squared absolute values of the wave functions for the model superlattices with $N_a = N_b = 15$, $p_a = -1$, $p_b = -3$ (a) and $N_a = N_b = 10$, $p_a = -1$, $p_b = 1$ (b).

$\psi_{c(v)a}$, $\psi_{c(v)b}$ and slowly-varying envelope functions $F_{c(v)}$. Two difficulties arise in calculating the band spectra of real superlattices using this method. The first is associated with the fact that the band-edge Bloch functions of semiconductors are often degenerate, requiring the use of multicomponent envelopes. In the 1D model under discussion here, this circumstance is nontrivial to model; therefore we limit ourselves to the two-band (Kane) approximation, which in 1D arises in a totally natural way.

The second difficulty is connected with boundary conditions. It is ordinarily assumed that the band-edge Bloch functions for the contacting materials are the same, and that the boundary conditions for the envelopes are derived in the effective-mass approximation, i.e., using conditions of the current-conservation form (see Ref. 13).²⁾ Although this approach is almost certainly invalid (it can only be partially justified for cases in which the properties of the contacting materials are identical in symmetry and when the lattice parameters of these materials are close), the results obtained using this method are usually (see, e.g., Ref. 12) in astonishingly good agreement both with experiment and with more refined theoretical calculations.

In this section we will discuss the second problem with the method of envelopes, i.e., the boundary-condition problem, using our 1D model. We will limit ourselves to the case $p_a p_b > 0$, since for $p_a p_b < 0$, i.e., for overlapping inverted bands, the solution is quite insensitive to the form of the boundary conditions, including the region of Tamm minibands. We will show that both the spectrum and the wave functions of the superlattice depend weakly on the form of the boundary conditions as long as we are not discussing interface (Tamm) minibands. Of course this is not surprising, since the latter generally do not appear when the envelope method is used with boundary conditions derived within the effective mass approximation. In order to obtain Tamm minibands in the envelope approximation, it is necessary to include discontinuities of the band-edge Bloch functions in the boundary conditions; indeed, these bands can appear only when the Bloch functions are different.

Returning to the model investigated in the previous section, we will seek the wave functions of the superlattice in the form

$$\Psi(x) = \begin{cases} F_c(x)\psi_{ca}(x) + F_v(x)\psi_{va}(x), & 0 < x < N_a \\ F_c(x)\psi_{cb}(x) + F_v(x)\psi_{vb}(x), & N_a < x < N_a + N_b \end{cases} \quad (11)$$

If the 2π gaps overlap for $p_a p_b > 0$ (as in Fig. 2a), it is necessary to use the same function for the Bloch functions of the bottom of the two upper bands (this is specific to the Kronig-Penney model with δ -functions):

$$\psi_c = 2^{1/2} \sin 2\pi x, \quad (12)$$

where the factor $2^{1/2}$ ensures unit normalization per unit length. Therefore in the present case $\psi_{ca} = \psi_{cb}$, and in fact no Tamm states appear near the upper bands.

On the other hand, the functions ψ_{va} , ψ_{vb} are different in this case, and have the form

$$\psi_{va}(x) = I_a \cos [(2\pi - \Delta_a)x + \Delta_a/2] \quad (13)$$

(in order to obtain ψ_{vb} it is necessary to replace the label a by

b). Here Δ_a is the width of the 2π gap (in units of ξ_a), and I_a is a normalizing factor that ensures normalization of (13) in the same way as (12).

To first order in $k \cdot p$ perturbation theory the equations for the envelope functions $F_{c,v}$ corresponding to the energy ε have the standard (Kane) form

$$(\varepsilon_{ca} - \varepsilon)F_c - i\Pi_a F_v' = 0, \quad (14)$$

$$-i\Pi_a F_c' + (\varepsilon_{va} - \varepsilon)F_v = 0,$$

where

$$\Pi_a = -i \int_0^1 \psi_{va}^* \psi_{ca}' dx$$

is the Kane parameter.

In order to obtain the wave function (11) and take into account the Bloch condition (9) it is necessary to correctly match the solution to Eq. (14) in layers of type A with the solution to the analogous equation (with replacement of label a by label b) in layers of type B . It is natural to use the condition of continuity of the wave function (11) and its derivative at the boundaries of layers A and B . We emphasize, however, that such boundary conditions³⁾ are usually not used, because they require knowledge of the exact form of the Bloch functions of the band extrema. In contrast, the boundary conditions of Bastard in the present case (first order $k \cdot p$ perturbation theory and the two-band approximation) have the form¹³

$$F_{vc}(x)|_{x=0-\delta} = F_{vc}(x)|_{x=0+\delta}, \quad F_{vc}(x)|_{x=N_a-\delta} = F_{vc}(x)|_{x=N_a+\delta}.$$

Note that because the Bloch functions ψ_{va} and ψ_{vb} are different, the exact boundary conditions introduce discontinuities in the envelope functions at the boundaries of the A and B lattices.

In Fig. 4 we compare the results of exact calculations of the superlattice spectrum (with the same parameters as in Fig. 2a) with approximate calculations using both the exact boundary conditions and Bastard boundary conditions. It is clear that the Tamm minibands are reproduced quite well in the envelope approximation. Again, this is not astonishing, since it is near the band edges that the Kane approximation works best.

If we use the Bastard boundary conditions, the solutions in the regions of localized and delocalized minibands are reproduced with good accuracy. However, as one might expect, the Tamm minibands disappear. The first miniband in the region of negative energies begins at $\varepsilon = 0$.

It is very interesting to investigate the approximate wave functions. In Fig. 5 we show the envelope functions (for the same values of the parameters as were used in Fig. 2a) calculated using the exact boundary conditions (a) and the Bastard boundary conditions (b). Despite the presence of discontinuities in the envelope functions in the first case and the absence of discontinuities in the second, the shapes of these solutions practically coincide for the upper bands. Differences of a nontrivial sort occur in the region of energies near the coincident valence bands of lattices A and B . For the case of Bastard boundary conditions, when $\varepsilon = 0$ and $K = 0$ (i.e., at the maximum of the uppermost negative-energy miniband) the envelopes have the obvious form

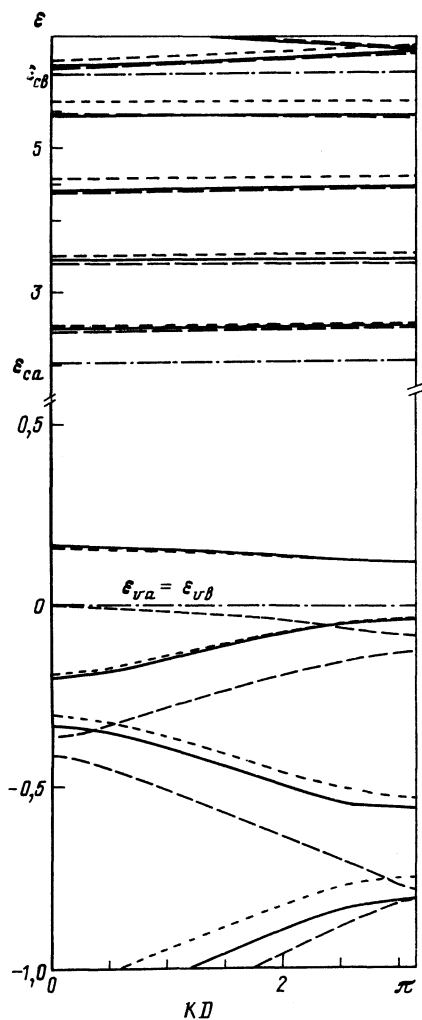


FIG. 4. The exact spectrum (short dashes), the spectrum calculated within the framework of the envelope approximation with exact boundary conditions (solid curves), and that calculated using Bastard boundary conditions (long dashes), for a superlattice with $N_a = N_b = 15$, $p_a = -1$, $p_b = -3$. The precision of the exact-boundary-condition approximation is very high for the special case of the Tamm miniband. Note carefully that the scale of energies in the region of the Tamm minibands has been expanded.

$F_v = 1$ and $F_c = 0$. This should also be true whether or not there are discontinuities in the valence band and Bloch boundary functions.

For the exact boundary conditions, the higher Tamm minibands (i.e., those located in the region of the forbidden energies common to both lattices) are essentially made up of valence-band wave functions ($|F_v| \gg |F_c|$), while both F_v and F_c decay into the depths of the layers. The shape of the lower Tamm minibands, which for these values of the parameters are located in a region of allowed energies common to both lattices, appears extremely nontrivial. Only one of the components (F_v) is localized at the interface. In addition, there is an extremely significant change in the upper bands as well: they are localized not at the interface but within the layers.

Although the spectrum of the Tamm minibands is very well described within the framework of the envelope approximation with exact boundary conditions (see Fig. 4), the description of the wave functions is considerably worse; in essence this is why the lower Tamm miniband behaves as it does when it lies in a region of allowed energies common to the bands of both lattices. This is abundantly evident from Fig. 6: the exact wave function is much more strongly localized than the approximate wave function. From this we may conclude that the Tamm miniband in the common region of allowed energies (of the bare spectra) arises as a result of a very precise balance of multiple scatterings of superlattice waves by the potential, which cannot be reproduced completely within the framework of the envelope approximation.

In conclusion we note the well known fact that the Tamm states are very sensitive to the form of the near-surface potential. Within the context of the model investigated here, this fact is clear, e.g., from Eq. (4): if in contrast to the present case we have $p_a < p_b < 0$, the Tamm states shift from the overlapping $2\pi n$ gaps to the $(2n + 1)\pi$ gaps; this also applies to the Tamm minibands in the superlattice. Therefore, one should not hope for a letter-perfect analogy between the present model and a real superlattice: the former is no more than a one-dimensional exactly-solvable

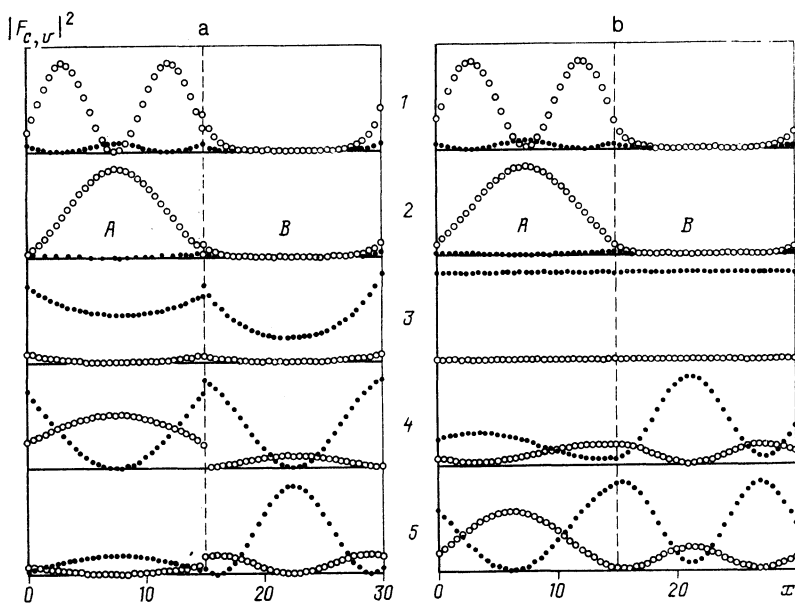


FIG. 5. Envelope functions calculated with the exact boundary conditions (a) and the Bastard conditions (b) for the same values of the parameters and E and K as in Fig. 2a: $\circ - |F_c|^2$, $\bullet - |F_v|^2$.

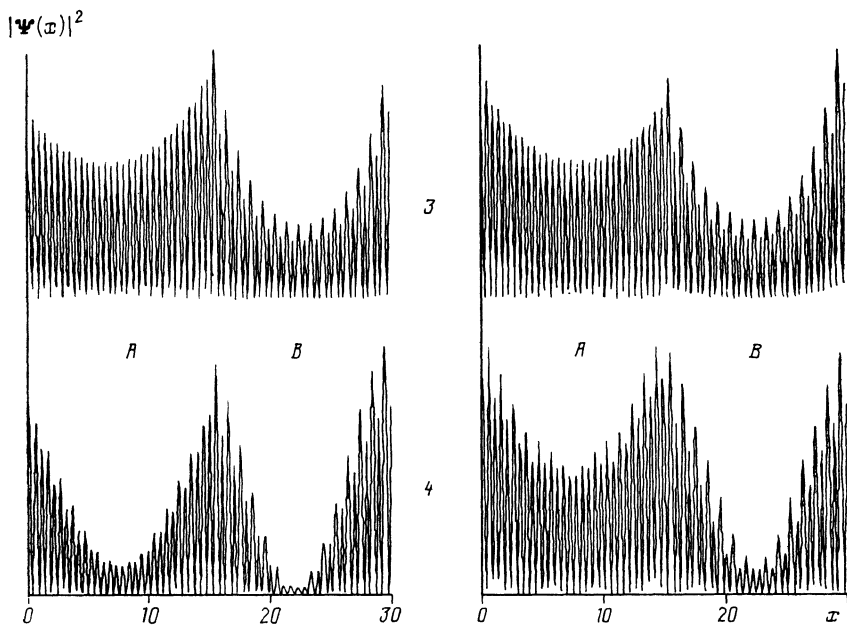


FIG. 6. A comparison of the exact wave functions (to the left) and those calculated within the envelope approximation with exact boundary conditions (to the right) for the Tamm minibands (at points 3 and 4 in Fig. 2a).

model in which there are Tamm levels and minibands. However, from our analysis of this model we may arrive at certain general conclusions. For example, if overlapping inverted bands are not involved, Tamm minibands can arise in superlattices with very different band-edge Bloch functions in neighboring superlattice layers, even in situations where these extrema are almost degenerate in energy. In this case it is not at all necessary for the periods of the adjacent layers to be different (in the model under investigation here we have purposefully chosen lattices that differ in their potentials but not in their periods). The interface minibands can be located in both allowed- and forbidden-energy regions that are common to both layers (for the bare spectra). The envelope approximation with Bastard boundary conditions describes the superlattice spectrum quite well if we overlook the absence of the Tamm minibands. In order to describe Tamm minibands within the envelope approximation, it is necessary (in the absence of band inversion) to include discontinuities of the Bloch functions of the extrema of the overlapping bands in the boundary conditions.

The author is grateful to N. A. Gippius for discussions and for pointing out the role of exact boundary conditions in the envelope approximation, and to L. V. Keldysh, V. V. Konopatskii, Yu. V. Kopaev, E. A. Mulyarov, and A. P. Silin for useful discussions and remarks.

¹⁾ As $N_{a,b}$ increases the overlap of wave functions of adjacent interfaces decreases, and the splitting of the Tamm minibands and their widths

decrease as well. Eventually the lower Tamm miniband is located in the gap region and the degree of localization ceases to depend on $N_{a,b}$.

²⁾ For brevity we will refer to these boundary conditions as the Bastard conditions.

³⁾ In what follows we will refer to them as the exact boundary conditions.

¹⁾ I. E. Tamm, *Zh. Eksp. Teor. Fiz.* [in Russian] **3**, 34 (1933) (see also I. E. Tamm, *Collected Scientific Works* [in Russian], Vol. 1, p. 216, Nauka, Moscow, 1975).

²⁾ C. Yia-Chang, J. N. Schulman, G. Bastard, Y. Guldner, and M. Voos, *Phys. Rev. B* **31**, 2557 (1985).

³⁾ N. A. Cade, *J. Phys. C* **18**, 5135 (1985).

⁴⁾ L. Quiroga, L. Camacho, A. Brey, and C. Tejedor, *Phys. Rev. B* **40**, 3955 (1989).

⁵⁾ B. A. Volkov and O. A. Pankratov, *Pis'ma Zh. Eksp. Teor. Fiz.* **43**, 99 (1986) [*JETP Lett.* **43**, 130 (1986)].

⁶⁾ W. Trzeciakowski, *Phys. Rev. B* **38**, 12493 (1988).

⁷⁾ N. F. Gashimzade, E. L. Ivchenko, and V. A. Kosobukin, *Fiz. Tekh. Poluprovodn.* **23**, 839 (1989) [*Sov. Phys. Semicond.* **23**, 526 (1989)].

⁸⁾ A. Alexandrou, L. L. Chang, and L. Esaki, *Phys. Rev. Lett.* **64**, 2555 (1990).

⁹⁾ M. Steslicka, R. Kucharczyk, and M. L. Glasser, *Phys. Rev. B* **42**, 1458 (1990).

¹⁰⁾ F. Agulló-Rueda, E. E. Mendez, H. Ohno, and J. M. Hong, *Phys. Rev. B* **42**, 1470 (1990).

¹¹⁾ S. G. Tikhodeev, *Pis'ma Zh. Eksp. Teor. Fiz.* **53**, 162 (1991) [*JETP Lett.*].

¹²⁾ D. L. Smith and C. Mailhot, *Rev. Mod. Phys.* **62**, 173 (1990).

¹³⁾ G. Bastard, *Phys. Rev. B* **25**, 7854 (1982).

Translated by Frank J. Crowne